Absolute Calibration of LLR Signal: Reflector Health Status

T. W. Murphy, Jr. [1], E. G. Adelberger[2], J. B. Battat[3], C. D. Hoyle[4], E. L. Michelsen[1], C. W. Stubbs[3], and H. E. Swanson[2]

1. UC San Diego, MC-0424, 9500 Gilman Drive, La Jolla, CA 92093-0424, USA;
2. University of Washington, MC-351560, Seattle, WA 98195-1560, USA;
3. Harvard University, Dept. of Physics, 17 Oxford Street, Cambridge, MA 02138, USA;
4. Humboldt State University, Dept. of Physics, Arcata, CA 95521, USA;

Abstract

The recently-operational APOLLO lunar ranging station has received lunar return signals as strong as 0.6 photons per pulse over short periods. This signal rate is high enough to allow system optimization and diagnoses that permit careful quantification of system performance. Moreover, observing a spatially flat part of the moon with a well-defined field of view yields a check on the total one-way system efficiency. We are therefore able to compare the lunar signal rate against theoretical expectations as a means of examining the health of the retroreflector arrays after 35 years or more in space. A key part of this analysis is a thorough understanding of the diffraction pattern returned by the corner cube array.

Introduction

Three of the Apollo lunar landing missions placed corner-cube arrays on the lunar surface for the purpose of laser range measurements. The arrays consist of identical 38 mm-diameter uncoated fused-silica corner cubes working via total internal reflection. The Apollo 15 array is three times larger than the first two (Apollo 11 and Apollo 14), making it the preferred target due to its higher return rate. Roughly 85% of laser range measurements to the moon utilize the Apollo 15 array. The present analysis concerns itself only with this array, though results from the others support our conclusions.

The photon count per pulse can be characterized by the link equation,

$$N_{\rm detect} = N_{\rm launch}\eta_{\rm c}^2\eta_{\rm r}\eta_{\rm NB}Qn_{\rm refl}\eta_{\rm refl}\left(\frac{d}{r\phi}\right)^2\left(\frac{D_{\rm eff}}{r\Phi}\right)^2, \qquad (1)$$

where $N_{\rm launch}$ is the number of photons emitted by the laser per pulse, $\eta_{\rm c}$ is the one-way optical efficiency common to both transmit and receive modes, $\eta_{\rm r}$ is the optical efficiency of the receiver, $\eta_{\rm NB}$ is the narrow-band filter peak transmission, and Q is the detector quantum efficiency. The reflector array is composed of $n_{\rm refl}$ corner cubes (300 for Apollo 15), each of diameter, d and efficiency $\eta_{\rm refl}$. The uplink beam has a divergence ϕ, while the downlink divergence is Φ. $D_{\rm ef}$ is the effective diameter of the telescope (such that the collecting area is $\pi D_{\rm eff}^2/4$, and r is the one-way distance between the telescope and the reflector array. The simplified link equation assumes "tophat" diffraction distributions rather than Gaussian or more complicated patterns as a rough estimate of flux in the center of the distribution. We will later abandon this simplification in a refined approach.

The sections below evaluate the terms in the link equation for the recently constructed APOLLO (Apache Point Observatory Lunar Laser-ranging Operation) apparatus [1], comparing the model to observed peak rates. First, the individual terms and their

errors are estimated, followed by a check of the one-way efficiency using the solar-illuminated lunar surface. Then the lunar return is estimated and compared to actual measurements. Ultimately, the calculation is modified to account for a realistic diffraction pattern from the lunar corner cubes. An attempt is made to propagate realistic errors throughout this analysis.

One-Way Throughput

The one-way throughput of the apparatus may be checked by looking at a star or other flux standard using the same detector path employed in detecting lunar laser returns. This checks the quantity $\eta_c \eta_r Q$ in the link equation.

The η_c and η_r terms are composed of a number of optical efficiencies, evaluating to 0.51±0.03 and 0.29–0.58, respectively. Atmospheric transmission, measured to be 0.87 for one airmass at 550 nm at Apache Point, is included in η_c. The large range on η_r stems from the fact that the APOLLO detector only spans 1.4 arcseconds on a side. Therefore, a point source above the atmosphere may overfill the array depending on atmospheric seeing. Despite the large range, given knowledge of the seeing we can estimate this parameter to ~10% precision, leading to a ~12% estimate on η_r. The detector quantum efficiency, *Q*, is roughly 0.30. This number matches theoretical expectations based on device structure, and the flux calibration to a flux standard is in agreement with this figure. The effective diameter of the Apache Point 3.5 meter telescope is 3.26 m.

For the purpose of estimating the one-way throughput when looking at a flux standard, we need to know that the effective bandpass of the narrow-band filter is $\Delta\lambda_{NB}$ = 0.95 nm, and that the integration time is Δt_{APD} = 95 ns per APD gate event. We use the flux calibration standard that a zero-magnitude source at 532 nm wavelength has a flux density of $F_0 = 3.9\times10^{-11}$ W m^{-2} nm^{-1}. The number of photons we see per gate event is then

$$N = \frac{\pi}{4h\nu} F_0 10^{-0.4m} D^2 \Delta\lambda_{NB} \Delta t_{APD} \eta_c \eta_r Q \,, \qquad (2)$$

where *m* is the stellar magnitude, and $h\nu$ is the photon energy. During full moon, we estimate the darker-than-average terrain around the Apollo 15 reflector to have a surface brightness of 3.60 magnitudes per square arcsecond. This translates to 2.87 magnitudes into the 1.4×1.4 arcsecond field of view. Accounting for the fact that only 13 of the 16 APD elements are operational, the expected lunar background rate is: $N_{lunar} = 0.40 \pm 0.08$ photons per gate. Comparing this to the measured full-moon background rate of 0.40 photons per gate, we claim to understand the one-way efficiency of our system. Similar analysis on a focused star yields similar results.

Lunar Return Rate

Simplified Calculation

Populating the terms in Equation (1), we take $\eta_{NB} = 0.35 \pm 0.025$, $N_{launch} = f_{launch} E_{pulse} / h\nu$, with $f_{launch} = 0.6 \pm 0.03$ as the geometrical loss of the Gaussian beam propagating out of the 3.5 meter telescope, and $E_{pulse} = 0.100$ J. Setting $n_{refl} = 300$, d = 0.038 m, $\eta_{refl} = 0.93$, $r = 3.85\times10^8$ m, $\phi = 0.8 \pm 0.12$ arcseconds, and $\Phi = 10 \pm 1.5$ arcseconds, we get an expected lunar return into the APD array (with its particular pattern of dead pixels) of: $N_{detect} = 12.0 \pm 6.1$ photons per pulse. If we use the information we get from the one-way system check, we

reduce the uncertainty by a small amount to ±5.6 photons per pulse.

Observed Lunar Return Rate

The APOLLO lunar return rate is highly dependent on atmospheric seeing and pointing. Not only does the illumination of the reflector scale as the inverse square of the seeing scale, the finite and small APD field of view truncates flux in poor seeing. Seeing of 2.0 arcseconds produces a return rate ten times smaller than at 1.0 arcseconds, if perfectly centered in both cases. For the present analysis, we use the two highest return rates observed in the first six months of APOLLO operation: 9 December 2005, and 17 January 2006. Both nights had exceptional seeing. On each night, we saw return rates of ≈ 0.5 photons per pulse over < 30 second intervals. In each case, telescope pointing and beam offset were optimized for the best signal.

The estimate of expected lunar rate above is 24 times the observed rate. Even though the analysis is a simplified version, the discrepancy is large, and difficult to eliminate through reasonable choices of parameters.

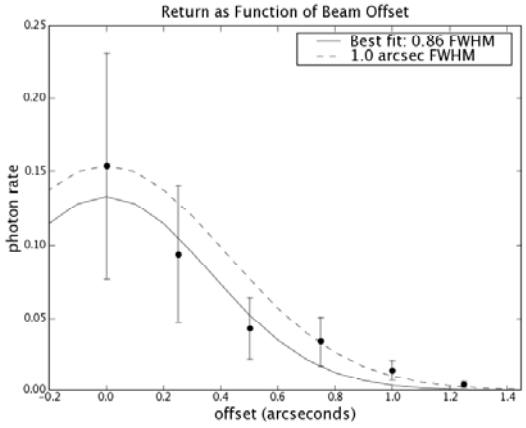

Figure 1*: Beam offset optimization on 9 Dec. 2005. At offset steps of 0.25 arcsec, it is clear that the beam size is less than 1.0 arcsec. Error bars are estimated at 50%.*

The effective beam size on the moon (affected by seeing and optical configuration) is the most obvious place to suspect poor understanding. As for the seeing, the median seeing at the Apache Point Observatory is 1.1 arcsec at zenith. Since the nights used for comparison had especially good seeing, we may assume the seeing to be less than 1.1 arcsec, and likely around 0.8 arcsec. But more convincingly, by rastering the beam pointing on the moon (while keeping the receiver fixed at the same location) we can demonstrate the sensitivity to beam offset, and see directly that the beam illumination footprint on the moon has a full-width at half-maximum (FWHM) less than one arcsecond (Figure 1). Though the best fit in Figure 1 is 0.86 arcsec FWHM, we have chosen 0.8 arcsec in the present analysis because the periods we have chosen for comparison represent the very best 30 second periods within ~10 minute runs. We therefore expect the conditions to have momentarily been better than the average for the run.

It should be noted that the multi-photon capability of APOLLO's detector array renders us insensitive to skewed statistics arising from the structure of the beam's speckle pattern on the moon. In the present analysis, some pulses are seen with as many as 6, 7, or 8 photons. We do not underestimate our return rate by missing these top-heavy events.

Refined Calculation

In the preceding analysis, we made the gross simplifying assumption that the beam patterns were uniform across a circular region—a so-called "tophat" profile. A more realistic calculation should:

- treat the outgoing beam as having a Gaussian profile;
- consider the theoretical diffraction pattern from a perfect corner cube;
- allow for manufacturing tolerance of the corner cubes;
- account for the reduced corner cube throughput as a function of incidence angle;
- de-rate the return strength due to thermal distortions of the corner cube;
- compensate for velocity aberration of the returning beam.

In this section, we treat each of these issues in turn, ultimately producing a more realistic estimate of the return rate, with less uncertainty.

A circularly symmetric Gaussian flux distribution has a peak irradiance that is ln2 ≈ 0.69 times the irradiance of a tophat whose diameter is the same as the Gaussian FWHM and carries the same total flux. Thus we multiply the return rate by this factor.

A corner cube prism employing total internal reflection (TIR) produces a diffraction pattern that is significantly different from that of an equivalent circular aperture. As seen in Figure 2, there is a central core of concentrated flux surrounded by a roughly hexagonal pattern containing significant flux. The core follows the Airy function that would be produced by a perfect circular aperture of the same diameter as the corner cube, but at a peak flux only 27% that of the Airy function, ignoring the two-way reflective surface loss. At normal incidence, the TIR pattern contains 36% of the total energy within the first Airy ring of radius $1.22\lambda/D$, where λ is wavelength and D is the diameter of the aperture [2]. This is compared to 84% for the Airy function.

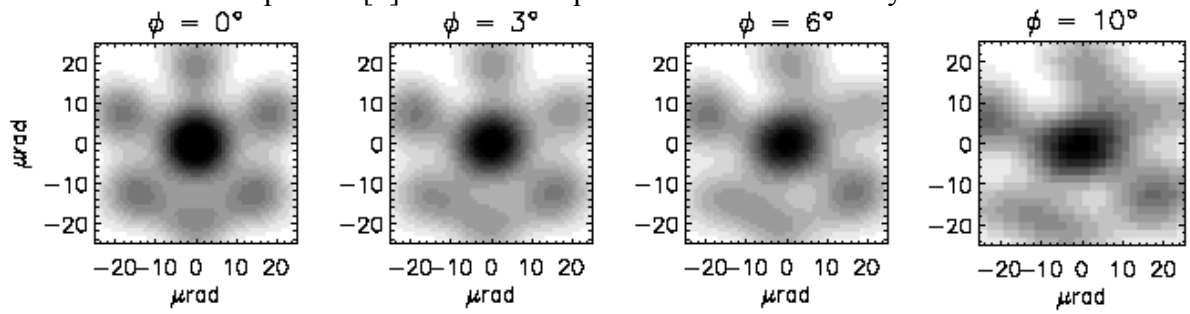

***Figure 2**: Sample diffraction patterns from an Apollo corner cube as a function of incidence angle. Data courtesy David Arnold.*

Compared to a tophat flux distribution with angular diameter λ/D, the normal-incidence TIR diffraction pattern has a central irradiance that is 0.182 times the tophat irradiance if both contain the same total flux. Including the 0.93 two-way front-surface reflection loss from fused silica (η_{refl}), the Apollo corner cubes produce a diffraction pattern with a central irradiance 0.169 times that of the comparison tophat. For the Apollo cubes and $\lambda = 532$ nm, the tophat diameter is 2.89 arcsec.

The manufacturing tolerance for the mutual perpendicular faces of the Apollo corner cubes was specified as ±0.3 arcsec [3]. It was reported that the central intensity of each corner cube selected for flight was at least 90% of the theoretical value. As such, we adopt a factor of 0.93 to provide a representative scaling of manufacturing imperfection.

Corner cubes have an effective cross section that is a function of the incidence angle. For circularly-cut fused silica corner cubes, this function is linear near normal incidence, with 4.3% loss per degree offset. In addition, the Apollo corner cubes are recessed in aluminum mounting structures by half their diameter, or about 1.9 cm. The recesses have conical flares, with half-angles of 1.5° for Apollo 11, and 6° for both Apollo 14 and 15. Together, these factors reduce the throughput by as much as a factor of two for the most extreme libration-induced tilts of 10° (Figure 3).

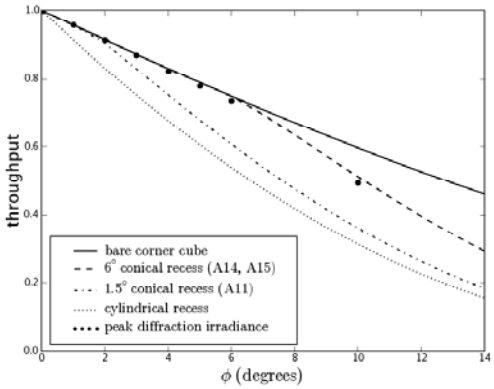

***Figure 3**: Corner cube throughput as a function of incidence angle and recess geometry. The single points come from diffraction patterns (as in Figure 2). Data courtesy Jim Williams.*

The thermal performance of the Apollo reflector arrays in the lunar environment was modeled and tested in great detail prior to flight. The primary performance degradation stems from thermal gradients within the corner cubes, which both deform the optical surfaces and present a refractive index gradient within the material—leading to distortion of the reflected wavefront [4]. For the Apollo 15 array, the central irradiance may be as low as 0.7 times the isothermal value. The original analysis presented plots of degradation as a function of sun angle for the three arrays, from which it is possible to evaluate the thermal degradation factor for any particular lunar phase [5].

Because the lunar reflector is in relative transverse motion with respect to the earth station—due both to the lunar orbit at ≈ 1000 m/s and earth rotation at ≈ 400 m/s—one must account for the angular shift in the diffraction pattern, amounting to $2\Delta v/c$. This amounts to 0.8–1.2 arcsec (4–6 μrad) depending on the vector sum of the relevant velocities. Given the functional form of the central region of the TIR corner cube diffraction pattern, this translates to a signal degradation of 0.64–0.86, or 0.75 on average.

Putting these factors together, we find that the response from the ideal TIR corner cube suffers a factor of 0.20–0.86 degradation. If one then treats the corner cube diffraction pattern as a λ/D tophat function, a pre-factor of 0.034–0.146 must be applied to the link equation. This is equivalent to a tophat function 8–15 arcsec in diameter with no degradation pre-factor.

Analysis of Two Cases

As mentioned before, we use two epochs—both at a return rate of 0.5 photons per pulse—to compare against the return estimate. Table 1 summarizes the various de-rating factors, and estimates resulting from the analysis. The squared atmospheric de-rating as a function of zenith angle has been included (belongs in η_c, technically).

The static factors shown in Table 1 represent the outgoing Gaussian beam profile, the TIR diffraction profile with surface reflection, and the manufacturing tolerance.

***Table 1**: De-rated return rate estimates for the two comparison epochs.*

Parameter	**Epoch 1 value**	**Epoch 1 de-rating**	**Epoch 2 value**	**Epoch 2 de-rating**
Velocity Aber.	1.09 arcsec	0.71	0.86 arcsec	0.81
Angular Offset	3.94°	0.84	4.04°	0.81
Sun Angle	–73°	0.85	35°	0.70
Range	371425 km	1.15	404301 km	0.82
Zenith Angle	50°	0.84	23°	0.97
Static Factors	0.69×0.169×0.93	0.108	0.69×0.169×0.93	0.108
Total de-rating		0.053		0.040
Return Estimate	8.2±3.4 phot./pulse		6.2±2.6 phot./pulse	
Estimate Ratio	16.4		12.4	

Using the de-rating estimates in Table 1 together with Equation (1), and taking the convention that $\Phi = \lambda/D = 2.89$ arcsec, we arrive at the conclusion that we see a return rate approximately 15 times weaker than expected. Given that the estimated net error is about 41%, and considering that this is a multiplicative problem, a one-sigma deviation would correspond to multiplying the estimate by (1 – 0.41) = 0.59. A two-sigma deviation corresponds to multiplying by $0.59^2 \approx 0.35$. To bring the discrepancy down to unity, we must be approximately five standard deviations away—a significant result.

To illustrate the robustness of this result, imagine that our estimate of the beam width—our least certain parameter—is less certain than our ±15% estimate. We could achieve the discrepant ratios by letting the beam profile be as large as 2.8–3.2 arcsec, which is not at all consistent with Figure 1, or APOLLO experience in general.

We conclude that the lunar reflectors have suffered performance degradation (ratios between reflectors are as expected) in their > 35 years on the lunar surface. We cannot tell whether the degradation is due to dust or surface abrasion. Recent work proposing a dynamic fountain of dust on the moon may be relevant [6].

References

[1] Murphy, T. W. et al., "APOLLO Springs to Life: Millimeter Lunar Laser Ranging," *Proceedings of the 15th International Laser Ranging Workshop*, Canberra, (2006)

[2] Chang, R. F., Currie, D. G., Alley, C. O., and Pittman, M. E., "Far-Field Diffraction Pattern for Corner Reflectors with Complex Reflection Coefficients," J. Opt. Soc. America, **61**, 431, (1971)

[3] Kokurin, Y. L., "Laser Ranging to the Moon," *Proceedings of the P. N. Lebedev Physics Institute*, **91**, p. 161

[4] Faller, J. E.., "The Apollo Retroreflector Arrays and a New Multi-lensed Receiver Telescope," *Space Research XII*, Akademie-Verlag, p.235, (1972)

[5] Faller, J. E. et al., "Laser Ranging Retroreflector," Chapter 14 of the NASA post-mission report on the Apollo 15 mission

[6] Stubbs, T. J., Vondrak, R. R., and Farrell, W. M., "A dynamic fountain model for lunar dust," *Advances in Space Research*, **37**, 59, (2005)